analytical chemistry

pubs.acs.org/ac Article

Sliding Windows in Ion Mobility (SWIM): A New Approach to Increase the Resolving Power in Trapped Ion Mobility-Mass Spectrometry Hyphenated with Chromatography

Hugo B. Muller, Georges Scholl, Johann Far, Edwin De Pauw, and Gauthier Eppe*

Cite This: *Anal. Chem.* 2023, 95, 17586−17594 Read Online

ACCESS | Metrics & More | Article Recommendations | Supporting Information

ABSTRACT: Over the past decade, the separation efficiency achieved by linear IMS instruments has increased substantially, with state-of-the-art IM technologies, such as the trapped ion mobility (TIMS), the cyclic traveling wave ion mobility (cTWIMS), and the structure for lossless ion manipulation (SLIM) platforms commonly demonstrating resolving powers in excess of 200. However, for complex sample analysis that require front end separation, the achievement of such high resolving power in TIMS is significantly hampered, since the ion mobility range must be broad enough to analyze all the classes of compounds of interest, whereas the IM analysis time must be short enough to cope with the time scale of the preseparation technique employed. In this paper, we introduce the concept of sliding windows in ion mobility (SWIM) for chromatography hyphenated TIMS applications that bypasses the need to use a wide and fixed IM range by using instead narrow and mobile ion mobility windows that adapt to the analytes' ion mobility during chromatographic separation. GC-TIMS-MS analysis of a mixture of 174 standards from several halogenated persistent organic pollutant (POP) classes, including chlorinated and brominated dioxins, biphenyls, and PBDEs, demonstrated that the average IM resolving power could be increased up to 40% when the SWIM mode was used, thereby greatly increasing the method selectivity for the analysis of complex samples.

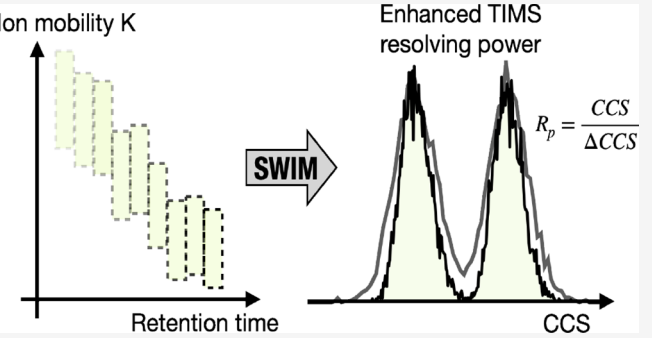

Downloaded via UNIV DE LIEGE on December 11, 2023 at 10:26:34 (UTC).
See https://pubs.acs.org/sharingguidelines for options on how to legitimately share published articles.

INTRODUCTION

Persistent organic pollutants (POPs) are toxic, persistent, and bioaccumulative industrial chemicals that are released (un)-intentionally in the environment and have raised global concern for both human and wildlife.[1] The Stockholm Convention, which came into force in 2004, aims to control the anthropogenic release of such contaminants in the environment and currently regulates over 34 harmful substances while three additional compounds are under review for potential inclusion.[2] All the chemicals listed in the convention, except one, are (poly)halogenated and include chlorinated (e.g., polychlorinated biphenyls PCBs, polychlorinated dibenzo-p-dioxins PCCDs), brominated (e.g., polybrominated diphenyl ethers PBDEs), and fluorinated (per- and polyfluoroakyl substances PFASs) compounds.[2] An increasing number of unregulated emerging persistent and bioaccumulative organic compounds are also being found in the environment.[3,4]

Standard protocols for monitoring halogenated POPs in various types of samples involve lengthy sample preparation steps followed by mass spectrometric analysis, typically preceded by chromatographic separations.[5] Due to the wide range of physicochemical properties displayed by different classes of POPs, a combination of LC and GC separations is usually required, with GC being the separation method of choice for (semi)volatile, nonpolar, and thermally stable analytes.[5] Moreover, complex samples usually contain many isomeric and isobaric analytes and interferences. To overcome this limitation, common approaches have been the use of an additional chromatographic dimensions such as in GC × GC,[6,7] high resolving power mass spectrometers,[8,9] and tandem mass spectrometry.[10]

Further selectivity can also be achieved with the inclusion of ion mobility (IM) after chromatographic separation and before mass spectrometer. Ion mobility is a gas phase separation technique that has recently shown great promise for the analysis of small molecules such as drugs,[11] biological compounds,[12,13] and chemical pollutants.[12] It separates ions based on their size, shape, and charge by dragging them through a buffer gas under the influence of an electric field.[14] Compared to chromatography hyphenated mass spectrometry,

Received: July 11, 2023
Revised: October 6, 2023
Accepted: November 3, 2023
Published: November 17, 2023

© 2023 American Chemical Society

https://doi.org/10.1021/acs.analchem.3c03039
Anal. Chem. 2023, 95, 17586−17594

IM offers two main advantages. First, it adds an additional "orthogonal" dimension of separation to mass-to-charge ratios and retention times, enabling the removal of some coeluting interferences and leading to cleaner MS and tandem MS spectra.[15] Second, the experimentally measured ion mobility can usually be converted to a collision cross-section (CCS) value, which is an intrinsic parameter of the analyte that is dependent on the experimental conditions. The CCS value can be compared to experimentally derived or in silico calculated values available in libraries and serve as an additional analyte identification point along with accurate mass, ion ratios, retention time, and tandem mass spectrum in both targeted[16,17] and untargeted approaches.[18,19]

Over the past decade, significant improvements have been made in the separation capability of IMS instruments.[20,21] While the resolving power (R_p) values of most commercially available IM-MS platforms rarely exceed 80,[22] state-of-the-art IM technologies, such as trapped ion mobility spectrometry (TIMS),[23] cyclic traveling wave ion mobility spectrometry (cTWIMS),[24] and structure for lossless ion manipulation (SLIM) platforms,[25] have demonstrated R_p values well over 200. These high resolving powers significantly improve overall separation capability[20] and accuracy in CCS determination.[26] However, achieving such high resolving powers in TIMS requires extended IM separation times and/or IM analysis over a restricted ion mobility range,[20] posing serious challenges for IM-MS applications that involve front-end chromatography to analyze compounds characterized by a broad range of CCS values in complex samples. For instance, while high resolving powers in the range of 150−400 have been achieved for singly charged ions in direct infusion mode,[27] R_p values below 100 have been more commonly reported for LC[28−30] and GC-TIMS-MS[31] applications. These values are of the same order of magnitude as the maximum resolving power that can be achieved on e.g., modern low-pressure drift tube IMS, which is considered as a lower resolving power technology.[20,21]

In this article, we report a new method of TIMS operation, called sliding windows in ion mobility (SWIM), to further increase the resolving power in hyphenation with front end chromatography without sacrificing the spectral acquisition speed. We provide a detailed description of the SWIM method and apply it to the analysis of complex standard mixture of 174 halogenated POPs. Besides, we focus on the ability of ion mobility to separate GC coeluting isomers and isobars. Indeed, although several papers have highlighted the potential of ion mobility for separating isomeric and isobaric species,[32−34] fewer have explored its utility when such species are poorly separated in the chromatographic dimension.[18,35,36] Finally, we discuss the trends in the GC, ion mobility, and m/z dimensions for the various classes of halogenated POPs analyzed in this study. Notably, we report the first IM analysis of several types of dioxins (PCDD/Fs, PBDD/Fs, and PXDD/Fs) and halogenated biphenyls (PBBs and PXBs), thereby contributing to the growing use of ion mobility for POPs[33,35,37,38] and other chemical pollutants in scientific research.[39−41]

EXPERIMENTAL SECTION

POP Standards Solution. Halogenated dioxins (PCDD/Fs, PBDD/Fs and PXDD/Fs), biphenyls (PCBs, PBBs and PXBs), and diphenyl ether (PBDEs) standards were purchased from Wellington (Ontario, CA) and CIL (Tewksbury, MA) and were mixed and diluted to a final concentration of 5−20 pg/μL in n-nonane (99%, Alfa Aesar). A detailed list of the 174 mixture constituents can be found in Table S1. Similarly, individual mixtures of 11 selected isomeric pairs were prepared in n-nonane (see Table S7). Additionally, standard mixtures of polycyclic aromatic hydrocarbon standards (PAHs), used for the ion mobility calibration procedure, polychlorinated naphtalenes (PCNs), and fatty acid methyl esters (FAMEs), were purchased from Wellington, CIL, and Merck, respectively.

GC-APCI-TIMS-MS Analysis. Measurements were performed on a commercial timsTOF Pro II mass spectrometer (Bruker, Bremen) equipped with a GC connected to an atmospheric pressure chemical ionization (APCI) source for sample introduction and ionization (GC-APCI II, Bruker, Bremen). Standard, SWIM, and UHR mode analyses were performed under the same experimental conditions as listed below, except for the TIMS parameters.

Injections were performed in splitless mode (injection temperature 275 °C, 1 μL) on a Bruker 456-GC equipped with a low polarity Rxi-5Sil MS column (30 m × 0.25 mm × 0.25 μm, Restek). A fast and linear GC oven temperature program was set in order to promote the coelution of isomers and isobars: 1 min 140 °C, 10 °C/min to 310 °C, hold 20 min, for a total analysis time of 38 min. Helium was used as the GC carrier gas at a flow rate of 2 mL/min. Under these conditions, the majority of the analytes were eluted within 20 min.

APCI of the analytes was performed in positive ionization mode and generated mostly stable radical molecular ions $M^{+\cdot}$, along with a smaller fraction of protonated $[M + H]^+$ ions (a detailed list of the ionization source parameters used is provided in Table S2).

TIMS separations were performed using nitrogen as the buffer gas (purity ≥99.999%). A complete list of specific parameters (voltages, pressure, and analysis times) used in standard, SWIM, and UHR modes is provided in Table S3. Importantly, the accumulation time in the storage section of the TIMS analyzer was optimized and set to 20 ms in order to avoid space charge effects[42] that drastically impacted the resolver power when longer trapping times were used (Figure S1). The qTOF analyzer was operated at 10 kHz in the range m/z 100−1000 in MS only mode (additional parameters are provided in Table S4). Mass calibration was performed using polysiloxane ions from the GC column bleed (Table S5).

All raw data processing was performed by using DataAnalysis (Bruker, version 5.3). Internal recalibration of both m/z and ion mobilities was performed after each data acquisition. Experimentally measured ion mobility values were converted to CCS values using the fundamental low-field (Mason-Schamp) equation, with T set arbitrarily to 305 K. Ion mobility resolving powers were calculated using the CCS-based definition[43] ($R_p = \mathrm{CCS}/\Delta_{\mathrm{fwhm}}\mathrm{CCS}$).

Ion Mobility Calibration. The mobility calibration procedure involved the use of 5 polysiloxanes ions that were present in the GC column bleed (Table S2). However, as reference CCS or $1/K_0$ values were not available in the literature for these ions, their CCS values were initially determined using a calibration method based on the reference stepped field $^{DT}\mathrm{CCS}_{N2}$ of polycyclic aromatic hydrocarbon (PAH) ions published in a database[33] (Figure S3). Using polysiloxane ions for IM calibration offers several advantages, including the coverage of a range of CCS values (approximately 140 to 200 Å^2) that is relevant to small molecules like POPs. Additionally, because they are background ions, the use

https://doi.org/10.1021/acs.analchem.3c03039
Anal. Chem. 2023, 95, 17586−17594

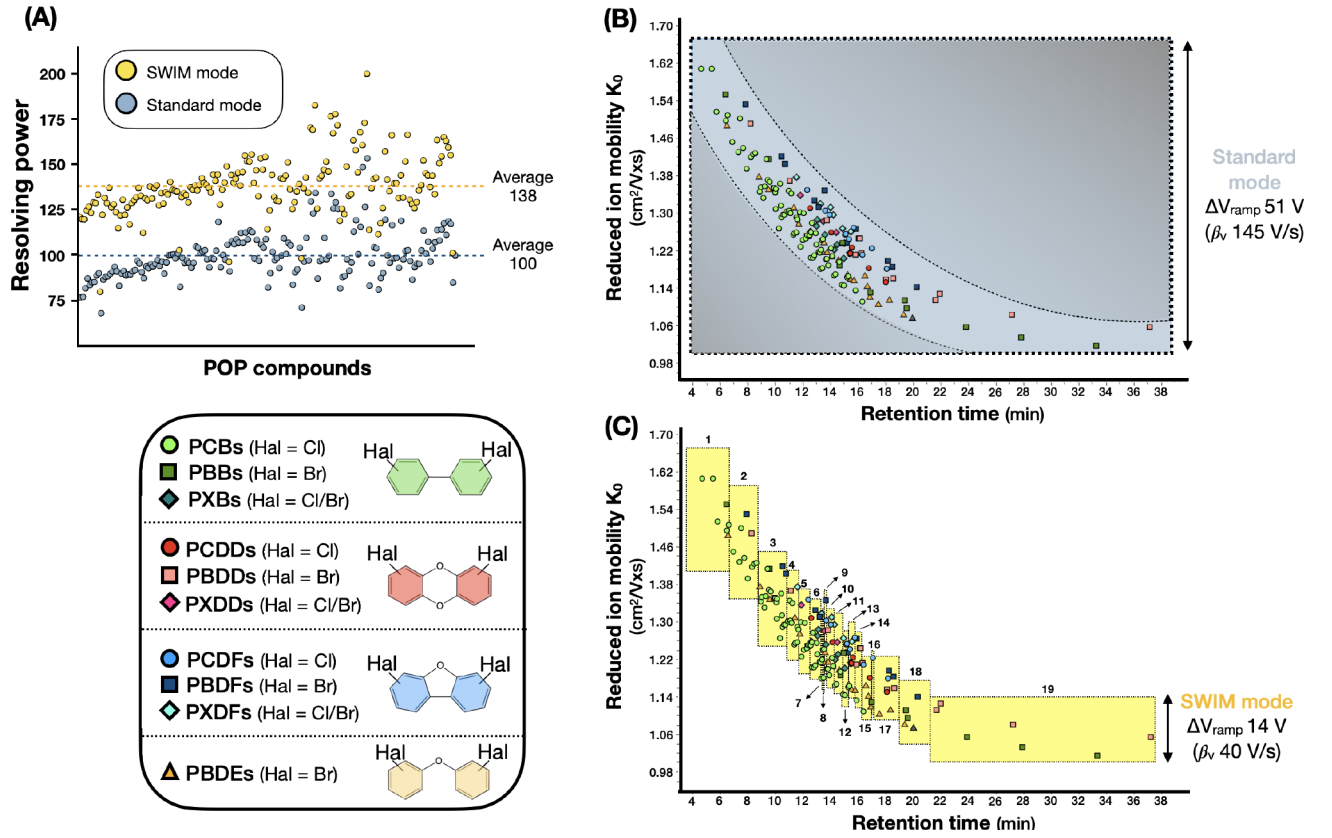

Figure 1. (A) Comparison of the individual IM resolving power of POPs (n = 174) achieved in standard (blue dots) and SWIM mode (yellow dots). (B, C) Experimentally measured reduced ion mobility values K_0 of POPs as a function of their GC retention time. In panel (B), the constant ion mobility range (between 1.00 and 1.66 cm^2/V s) that was used throughout the gas chromatographic separation in standard mode is represented by the blue rectangle. The dotted curves have been added to highlight the observed end of decreasing ion mobilities with increasing retention times. In panel (C), the 19 "ion mobility windows" that were used in SWIM mode are represented by yellow rectangles. The inset below panel (A) provides an overview of the general structures and names of the types of POPs analyzed in this study.

(and purchase) of an auxiliary calibrant (e.g., Agilent tune mix) is avoided, and internal recalibration of the data can be performed after each acquisition to achieve the best reproducibility in CCS measurements.

RESULTS AND DISCUSSION

Resolving Power in GC-TIMS. Trapped ion mobility (TIMS) is a modern type of time-dispersive ion mobility technique where ions are initially separately trapped in an electrical field and subsequently released by order of decreasing CCS to the mass analyzer.[44] Briefly, ion trapping is achieved by using an increasing electric field gradient (EFG) to counteract the drag force exerted from a moving gas. Because ions of higher CCS experience a higher drag force compared to lower CCS ions, they will reach an equilibrium position further up the EFG, where the electric field is higher. Sequential elution of the trapped ions by the order of decreasing CCS is then achieved by progressively lowering the electric field gradient.

In TIMS, the resolving power (R_p) has been shown theoretically and experimentally to depend mainly on the ramp speed β_v (i.e., the rate at which the voltage is decreased during the elution step) and the drift gas velocity v_g, as shown in a simplified form in eq 1.[45−47] While increasing gas velocity can greatly improve resolving power, it can also lead to complications at higher flow rates, as reported in the literature.[46] As a result, gas velocity is typically kept at the default value set by the manufacturer (such that $V_{elution}$ of $[M + H]^+$ ion of hexakis(2,2-difluoroethoxy)phosphazine = 132 ± 1 V). Instead, adjusting the ramp speed is the primary means of fine-tuning the resolving power to meet the needs of a particular TIMS application. This flexibility is enabled by the unique "trap and release" scheme of the TIMS experiment, which allows ions within a selected mobility range to be selectively trapped and mobility analyzed for a user-defined time. This remarkable feature enables the use of shorter ion mobility ranges (ΔV_{ramp}) and/or longer analysis times (t_{ramp}) to achieve decreased ramp speeds ($\beta_v = \Delta V_{ramp}/t_{ramp}$) and increased resolving powers for the analytes of interest (as described by eq 1). Other experimental parameters that also significantly impact the resolving power and require careful optimization are the RF confinement amplitude[47,48] and the ion density at the position of trapping[42] (i.e., the number of ions accumulated in the TIMS analyzer).

$$R_p \propto \frac{v_g}{\sqrt[4]{\beta_V}} \quad (1)$$

While the flexibility of TIMS to tune the separation efficiency allows the achievement of high resolving power in direct infusion IM-MS mode by setting a combination of long analysis time and short ion mobility range,[27−29] the use of slow scan rate is compromised when (1) relatively fast coupling front end separation techniques, such as liquid and, specifically, gas chromatography, prevent the use of arbitrarily long analysis

https://doi.org/10.1021/acs.analchem.3c03039
Anal. Chem. 2023, 95, 17586−17594

time (2) target analytes possess a broad range of CCS values, requiring the use of an extended ion mobility range.

For instance, in this work, the chromatographic peaks had a baseline elution width of about 4 s, which limited the maximum analysis time to approximately 350 ms in order to ensure adequate sampling of each peak (about 11 TIMS separations per peak, Figure S4). Additionally, the compounds of interest displayed a wide range of CCS values, from as low as 133 Å^2 (for 2-chlorobiphenyl, a singly chlorinated biphenyl) to as high as 200 Å^2 (for the decabrominated biphenyl PBB 209), requiring a minimum trapping voltage range (ΔV_{ramp}) of 51 V. Under these constraints, the analysis of the POPs mix achieved an average resolving power of 100 (average CCS_{fwhm} 1.7 Å^2), as shown in Figure 1a, which is comparable to the R_p obtained in other TIMS studies using a similar scan rate (β_v = 51/0.350 = 145 V/s)[30,31] and already higher than most R_p values reported for DTIMS and linear TWIMS instruments for these types of compounds.[33,49]

Concept of SWIM. As discussed in the previous section, the diverse range of CCS values displayed by the different pollutant classes required the use of a relatively wide ion mobility range (ΔV_{ramp} = 51 V). However, upon examination of the ion mobility versus retention time profiles of halogenated POPs (Figure 1b), it becomes clear that the use of such a broad and fixed ion mobility range throughout the chromatographic separation ("standard TIMS mode", blue rectangle) does not efficiently trap and analyze the compounds of interest. Indeed, as depicted in the figure, the analytes tend to elute in an orderly, rather than random, manner, from higher ion mobilities (low CCS) to lower ion mobilities (high CCS), such that at any given retention time, the compounds of interest that elute from the GC column and enter the TIMS cell are characterized by a range of ion mobilities that is only a small fraction of the total ion mobility range actually covered by all these pollutants. Consequently, a significant portion of a given TIMS scan, and thus valuable analytical effort, is spent analyzing ion mobility regions that do not contain the targeted analytes (shaded areas), thus limiting the achievable resolving power.

The clear correlation of decreasing ion mobilities with increasing retention times observed in Figure 1b can be attributed to the relationship between the halogenation degree and both retention time and CCS in halogenated compounds. Specifically, as the degree of halogenation increases, so do the boiling point (RT) and size (CCS) of the compounds (Figure S5). As a result, compounds with lower halogenation degrees, characterized by lower CCS values, tend to elute before those with higher degrees of halogenation and higher CCS values.

Based on these correlations, we developed the concept of sliding windows in ion mobility (SWIM), which is depicted in Figure 1c. The rationale of SWIM is to divide the total analysis time of the GC run into small retention time segments that are each configured to trap and analyze ions within a narrow range of ion mobilities that effectively match those of the compounds of interest eluting during that time window. Technically, this can be achieved since in TIMS, the voltages on the different electrodes of the tunnel can be independently adjusted for each retention time segment in order to only trap and separate ions with the desired range of ion mobilities. We refer to these narrow ion mobility ranges as "ion mobility windows" that "slide" and adapt to the elution profile of the targeted analytes throughout the gas chromatographic analysis, hence the name of the concept. A small guide on how to implement the SWIM method on commercially available TIMS instruments using the timsControl software is given in the Supporting Information.

By using narrower IM ranges at a time, the scan rate is decreased, thereby enhancing the separation power.[45] This is indeed what was observed experimentally on a mixture of halogenated POPs. Based on the ion mobility vs retention time profile of these compounds, the GC run was divided into 19 segments, each optimized to selectively separate the ions of interest (Figure 1c and Table S6, see also guide in the SI). The first IM windows were set to selectively analyze the more volatile and lower CCS pollutants. Then, they were set to gradually analyze the higher boiling points and higher CCS compounds. This "SWIM mode" enabled a nearly 4-fold decrease in the scan rate (40 V/s, with ΔV_{ramp} = 14 V and t_{ramp} = 350 ms) compared to the traditional "standard mode", which used a wider and fixed ion mobility range. This resulted in a ∼40% increase in the average resolving power (on the order of 138, average CCS_{fwhm} 1.2 Å^2, Figure 1a). Moreover, this result is consistent to the expected ∼40% enhancement in R_p based on theory and eq 1 for such a decrease in scan rate ($R_{p\ SWIM}/R_{p\ Std} \simeq \sqrt[4]{145/40} = 1.4$). Importantly, the SWIM method did not affect the accuracy of the experimentally measured CCS values (average absolute ΔCCS of 0.07%, Figure S6) or the signal intensity (Figure S7) compared to that of the standard mode of operation.

Interestingly, the concept of segregating the chromatographic analysis into several retention time segments shares similarities with the chromatographic segments commonly employed for the single ion monitoring (SIM) and multiple reaction monitoring (MRM) of POPs such as dioxins and PCBs on "high" resolution magnetic sector[50] and triple quadrupole[51] mass spectrometers, respectively. However, while in these methods, the different chromatographic segments are configured to isolate ions based on their m/z ratio, in SWIM, they are configured to isolate ions based on their ion mobilities (i.e., CCS), regardless of their mass. Furthermore, it is worth noting that that the concept of scanning the ion mobility range of interest in TIMS using narrow ranges of trapping voltages has been previously investigated with the oversampling accumulation (OSA)[52] and gated TIMS[53] modes of operation. These modes employ small elution steps and nonlinear scans to selectively transmit ions of narrow ion mobility range at a time. Both types of experiments were developed to allow the hybridization of TIMS with slow mass analyzing FT-ICR instruments. Overall, the present SWIM concept can therefore be thought of as a hybrid method that incorporates both the concepts of chromatographic segments in GC-HRMS and GC-QqQ and scanned trapping IM range in OSA and gated TIMS.

Finally, it should be mentioned that the ion mobility windows in SWIM differ from those used in parallel accumulation-serial fragmentation (PASEF) methods[54−56] in that they are based on the isolation of a narrow range of ion mobility during a given chromatographic retention time whereas those in PASEF are based on the isolation of a narrow m/z range during a given ion mobility "elution time".

(HR)IM of Coeluting Isobaric and Isomeric POPs. The identification and quantification of pollutants in complex samples using chromatographic-based MS analysis remains a significant challenge due to the occurrence of coeluting isobars and isomers.[41,57,58] Coeluting isobars, which have the same nominal mass, require high mass resolving power or tandem MS for differentiation, while coeluting isomers cannot be

https://doi.org/10.1021/acs.analchem.3c03039
Anal. Chem. 2023, 95, 17586−17594

distinguished if they have identical or similar fragmentation spectra.[18,49] This problem is particularly pronounced for halogenated POPs, which exhibit a wide diversity of isomeric and isobaric congeners. In our study, although most pollutants were fully resolved in the GC and/or m/z dimensions (78%), we observed a considerable fraction of coeluting or partially coeluting isobars and isomers (10% and 12%, respectively).

One notable example of such coelution was observed with the partially coeluting isomeric PeCBs (84, 90, and 101, m/z = 325.8799) and the isobaric DiBDF (2,4-DiBDF, m/z = 325.8760), as shown in Figure 2a. The small mass difference

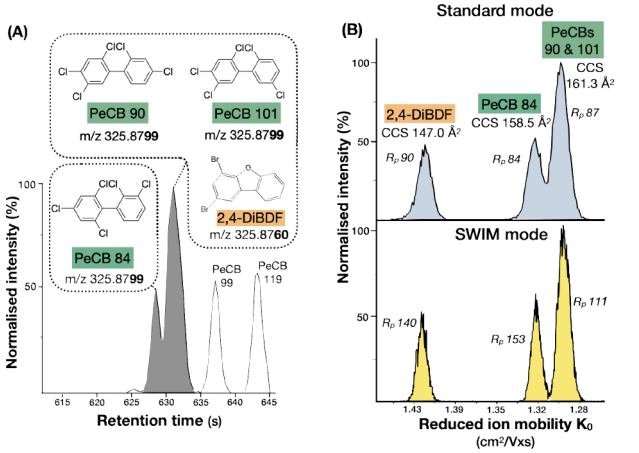

Figure 2. (A) GC chromatogram of pentachloro biphenyls (PeCBs) and dibromodibenzofuran (DiBDFs) highlighting the (partial) coelution of PeCBs 84, 90, and 101 (isomers) and 2,4-DiBDF (isobar). (B) Corresponding ion mobility spectra in standard mode (upper spectrum) and SWIM mode (lower spectrum).

($\Delta m/z = 3.9 \times 10^{-3}$) between these species required a mass resolving power on the order of 84,000 to achieve complete resolution in the m/z dimension. However, the resolving power of the TOF spectrometer used in this study (~50,000) was not sufficient to achieve this separation. Consequently, none of the four species could be fully resolved in either the GC or the m/z dimension in this specific case.

However, the ion mobility dimension provided additional separation, as depicted in Figure 2b. In standard mode (upper mobility spectrum), the radical $M^{+\cdot}$ ion of the dibromo-substituted furan was clearly distinguished from the three isomeric pentachloro substituted biphenyls due to the notable differences in halogenation degree (2 bromine vs 5 chlorine atoms), which resulted in considerable differences in CCS (>7%). On the other hand, for the three isomeric PCBs, only partial separation was achieved between the partially coeluting PeCB 84 and PeCBs 90−101, while no distinction was noted for the latter isomeric pair (that perfectly coeluted in the GC dimension). However, in SWIM mode (lower mobility spectrum in Figure 2b), baseline separation of PeCB 84 from PeCBs 90−101 was achieved, owing to the increased separation efficiency provided by this method. Nonetheless, isomeric PCBs 90 and 101 still appeared as a single peak in the mobility spectrum, despite the increased resolving power.

The example discussed above provides clear evidence of the added value of ion mobility as an additional dimension of separation for critical isobaric pairs. In fact, we observed that all of the other (partially) coeluting isobaric species could be separated at the baseline in the ion mobility dimension, even with the lower resolving power provided by the standard TIMS method (Figure S8). They reflect the fact that despite having nearly identical mass, these POP isobars possess significantly different three-dimensional structures due to variation in the central aromatic part, number, and type of halogen atoms.

However, for the majority of the (partially) coeluting isomeric pairs, the corresponding ion mobility spectra were characterized by a single, convoluted peak in both the standard and SWIM modes (Figure S9), except in two cases (HxCBs 128−167 and PeCBs 84−91/101) where partial (standard mode) and baseline (SWIM mode) separations were achieved (Figures S9H and 2b).

To further assess whether these isomeric pairs could be resolved at still higher resolving powers, standard mixtures of each pair were injected individually and analyzed in ultra high resolution (UHR) TIMS mode by setting the IM range to its lowest value (ΔV_{ramp} = 3.5 V) in order to reach the lowest scan rate (10 V/s, with t_{ramp} = 350 ms, Table S3 and S7) and the highest resolving power. The resulting ion mobility spectra of the different isomeric pairs are depicted in Figure 3 and Figure

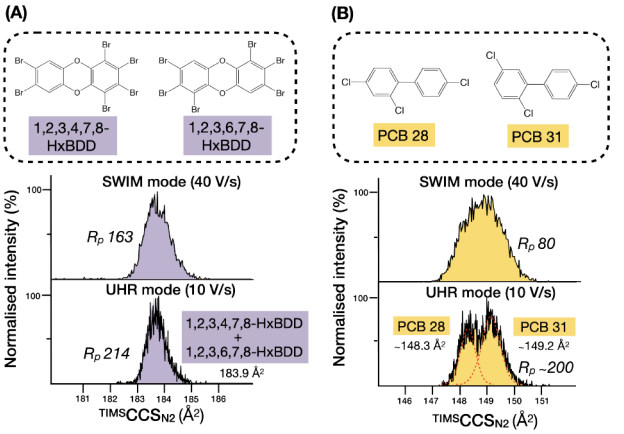

Figure 3. Trapped ion mobility spectra of the GC coeluting isomeric pairs 1,2,3,4,7,8 and 1,2,3,6,7,8-hexabromodibenzodioxins (A) and trichlorobiphenyls 28 and 31 (B) acquired in ultrahigh resolving power mode (β_v = 10 V/s), using very narrow IM ranges centered on the IM values of the corresponding isomeric pairs (Table S7). The corresponding ion mobility spectra obtained in the SWIM mode (β_v = 40 V/s) were added on top for comparison. Gaussian fits have been added in (B) to highlight the partial isomer separation achieved in UHR mode.

S10. As shown in these figures, hardly any improvements were noted in the separation of these isomers compared to the standard and SWIM modes in spite of the increased separation power provided by this lower scan rate (Figure 3a and Figure S10). Only one exception was noted for the case of the PCBs 28−31 pair, where partial separation was achieved (Figure 3b). Based on this result, the percent difference in CCS was calculated to be no greater than 0.6%. Given that both PCBs are positional isomers whose structures differ only in the position of a single chlorine atom, this small difference in CCS is not surprising. According to the model developed by the group of McLean et al.,[59] baseline separation of these two PCB isomers would require an ion mobility resolving power of approximately 350, nearly three times that achieved with the current SWIM mode (scan rate of ~40 V/s) and four times that reached in standard mode (scan rate of ~150 V/s). For the other isomeric pairs in Figure 3a and Figure S10, the

https://doi.org/10.1021/acs.analchem.3c03039
Anal. Chem. 2023, 95, 17586−17594

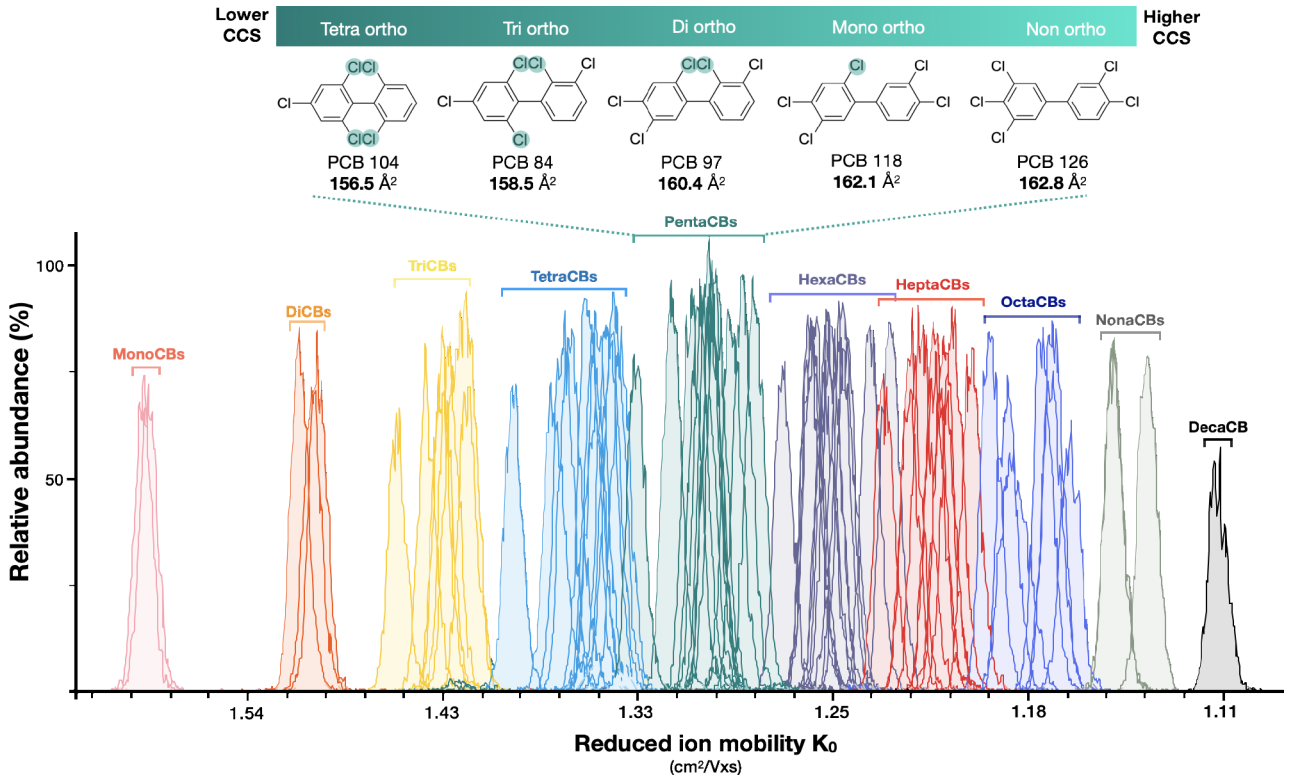

Figure 4. Overlaid ion mobility spectrum of the 82 PCBs analyzed in this work. The inset illustrates the trend of decreasing CCS with increasing chlorine substitution at the ortho positions for a few selected pentachlorobiphenyl isomers.

resolving power required to separate them would still need to be higher since they are characterized by even smaller differences in CCS, if any.

Some Trends in the CCS, Mass, and RT of Halogenated Aromatic POPs. When using traditional apolar GC stationary phases like DB5, halogenated POP compounds are typically primarily separated according to their degree of halogenation, from lower to higher halogenation degree, while further separation of isomers having identical number of halogen substituents depends on the substitution pattern of these halogen atoms.[60] Interestingly, a similar pattern was noted in this work in the ion mobility dimension for all the classes of POPs investigated. Figure 4 demonstrates this relationship for the class of PCBs. As shown in this figure, the congeners are also primarily separated according to their halogenation degree. This is due to the considerably larger size of chlorine atoms compared to hydrogen atoms.[19] Then, within a given halogenation degree, the PCB isomers also appear to be further separated based on the substitution pattern of chlorine atoms on the biphenyl moiety. In particular, as previously reported in the literature, PCB isomers exhibit lower collision cross section values as the extent of substitution at the ortho position increases.[33] This trend is likely due to the adoption of a more compact conformation by noncoplanar PCBs compared to more extended coplanar, dioxin-like PCBs. This pattern was also observed for the corresponding brominated biphenyl (PBB) isomers analyzed in this study (Figure S11). An interesting similarity can be observed between this specific trend and the relative GC retention time of the PCB isomers. In both cases, a higher extent of ortho substitution leads to lower retention times in GC and lower CCS values in IM analysis[61] (Figure S12).

CCS trends according to substitution patterns were also observed for isomers belonging to other classes of POPs. For example, in the case of hexa 2,3,7,8 substituted dibenzodioxins (PCDDs and PBDDs), isomers having the two extra halogen atoms on opposite sides of the dibenzodioxin moiety displayed higher measured CCS compared to those having them on the same side (Figure S13). Similarly, for the corresponding penta- and hexa-2,3,7,8-substituted dibenzo furans (PCDFs and PBDFs), isomers with extra halogen atom(s) on the same side of the dibenzofuran moiety as the oxygen atom (positions 4 and 6, Figure S14) generally displayed higher CCS values. This could be attributed to the fact that halogens in those positions lead to more extended structures compared to halogens in positions 1 and 9 (on the opposite side of the oxygen atom).

Finally, we observed that each class of halogenated POPs analyzed in this study displayed distinct trend lines in the CCS vs m/z dimension (Figure S15a), which is consistent with previous studies on PCBs, PBDEs, and PAHs.[19,33] Notably, we observed a clear segregation of the trend lines between brominated POPs, chlorinated POPs, and the nonhalogenated class of PAH pollutants, which can be attributed to the higher mass density of molecules bearing halogen atoms,[19,37,39] particularly brominated atoms.[49] As discussed in recent study by Baker et. al,[19] these specific m/z vs CCS trendlines can be used as an additional data prefiltering tool to conventional mass defect filtering in nontargeted applications. As expected, dioxins and biphenyls substituted with both chlorine and bromine atoms (PXDD/Fs and PXBs, respectively) were located in between the chlorinated and brominated regions (Figure S15b), with CCS values increasing with a higher bromination degree (Figure S16). Also, our data revealed that for a given halogenation degree, the relative CCS of different

https://doi.org/10.1021/acs.analchem.3c03039
Anal. Chem. 2023, 95, 17586−17594

classes of chlorinated and brominated POPs roughly followed the order $CCS_{Dibenzodioxins} \simeq CCS_{Diphenyl\ ethers} > CCS_{Dibenzofurans}$ (Figure S17. Halogenated biphenyls exhibited an average CCS lower than that of other POPs classes for lower halogenation degrees ($n \leq 4$) but gradually became comparable to that of halogenated dibenzofurans ($5 \leq n \leq 7$) and halogenated dibenzodioxins/diphenyl ethers ($n = 8$) as the halogenation degree increased. This was evident from the higher rate of CCS increase with increasing halogenation degree of halogenated biphenyls compared to the other classes, as shown by the dotted curves in Figure S17.

CONCLUSIONS AND PERSPECTIVES

This paper presented a novel approach for increasing the resolving power of TIMS in hyphenation with front end chromatography, known as SWIM, without compromising the spectra rate, duty cycle, sensitivity, or CCS measurement accuracy. The method was applied to a mixture of 174 POPs standards and resulted in a significant (~40%) improvement in resolving power compared to the standard TIMS mode.

Furthermore, a focus on the GC coeluting isobaric and isomeric species of this mixture revealed that ion mobility is a powerful tool to discriminate coeluting isobars, even at moderate resolving powers of around 100. However, it was noted that most coeluting isomeric POPs could not be separated even when the instrument was operated in ultrahigh resolution ion mobility (UHRIM) mode at $R_p \sim 200$, owing to their very small difference in CCS. The newly introduced cyclic and SLIM TWIMS platforms have shown exceptionally high resolving power up to 750[24] and 1860,[62] respectively, but the achievement of such ultrahigh resolving power for front end chromatographic hyphenation applications is yet to be demonstrated.[37,63,64]

Although the SWIM method is rather targeted in its implementation (i.e., the ion mobility windows are set based on the CCS vs RT profile of the analytes of interest, see guide in the SI), given the similar trends of ion mobilities vs retention time observed for the different subclasses of halogenated POPs, it is highly likely that other analogous subclasses that were not initially targeted during the IM windows optimization may exhibit a similar trend in the IM vs RT space and be included in the set windows, opening the possibility of performing suspect or even untargeted screening on these other subclasses of halogenated POPs. For example, a separate analysis of a mixture of polychlorinated naphthalenes (PCNs) standards showed that they followed the same general K_0 vs RT trend as that of the other subclasses of halogenated POPs (Figures S19).

Moreover, while in the current study, the SWIM method was successfully applied to several subclasses of GC amenable halogenated persistent organic pollutants, it has the potential to be applied to other classes of compounds and front-end separation techniques, including liquid chromatography or electrophoretic techniques. Indeed, the SWIM mode is applicable to classes of compounds that exhibit a specific trend in the ion mobility (i.e., CCS) versus retention time space. Such trends were clearly demonstrated for the different subclasses of chlorinated and brominated POPs in this study (10 subclasses in total). However, we also observed that there was a similar correlation for a mixture of saturated and unsaturated fatty acid methyl esters (FAMEs, Figure S18). Moreover, in the literature, other classes of compounds were also found to display such characteristic trends, including PFAS,[35] PBDE metabolites,[65] and PAHs.[31] Yet, plots of CCS/drift time vs RT for pesticides in two studies showed a much poorer correlation[17,40] (although a general increase in CCS/drift time with RT was still noticeable), probably due to the fact that the class of pesticides presents a much higher degree of chemodiversity compared to the homologous classes of compounds investigated in this study. The recent availability of predictive models for both retention times[66] and CCS[67] could help in assessing the potential implementation and openness of the SWIM methodology to various classes of compounds in food and environmental and biological matrices.

ASSOCIATED CONTENT

Supporting Information

The Supporting Information is available free of charge at https://pubs.acs.org/doi/10.1021/acs.analchem.3c03039.

Additional APCI, TIMS and MS settings; ion mobility windows settings; impact of accumulation time on resolving power; ion mobility calibration procedure; sensitivity and CCS accuracy of the SWIM method; additional IM spectra of (partially) coeluting isobars and isomers; additional RT, m/z and IM trends of POPs (PDF)

SWIM user guide (PDF)

List of the halogenated POPs analyzed in this study and their measured $^{TIMS}CCS_{N2}$ (PDF)

AUTHOR INFORMATION

Corresponding Author

Gauthier Eppe − *Mass Spectrometry Laboratory, University of Liège, Liège 4000, Belgium;* orcid.org/0000-0002-4821-3115; Email: g.eppe@uliege.be

Authors

Hugo B. Muller − *Mass Spectrometry Laboratory, University of Liège, Liège 4000, Belgium*

Georges Scholl − *Mass Spectrometry Laboratory, University of Liège, Liège 4000, Belgium*

Johann Far − *Mass Spectrometry Laboratory, University of Liège, Liège 4000, Belgium;* orcid.org/0000-0003-1208-6262

Edwin De Pauw − *Mass Spectrometry Laboratory, University of Liège, Liège 4000, Belgium;* orcid.org/0000-0003-3475-1315

Complete contact information is available at: https://pubs.acs.org/10.1021/acs.analchem.3c03039

Author Contributions

The authors confirm contribution to the paper as follows: study conception and design: H.B.M., G.S., J.F., E.D.P., and G.E.; data collection: H.B.M.; analysis and interpretation of results: H.B.M., G.S., J.F., E.D.P., and G.E.; draft manuscript preparation: H.B.M.; funding acquisition: G.E. All authors reviewed the results and approved the final version of the manuscript.

Notes

The authors declare no competing financial interest.

ACKNOWLEDGMENTS

This publication was supported by the French Community of Belgium through the funding of a FRIA grant (FC 47331). The authors also thank Bruker for their support and the Belgian

Federal Public Service of Health, Food Chain Safety and Environment through the contract RT22/06 TEQFOOD.

REFERENCES

(1) Jones, K. C.; de Voogt, P. *Environ. Pollut.* **1999**, *100* (1−3), 209−221.
(2) *Listing of POPs in the Stockholm Convention*. http://www.pops.int/TheConvention/ThePOPs/AllPOPs/tabid/2509/Default.aspx (accessed 2023−05−08).
(3) Muir, D. C. G.; Howard, P. H. *Environ. Sci. Technol.* **2006**, *40* (23), 7157−7166.
(4) Kumar, A. R.; Singh, I.; Ambekar, K.; Kumar, A. R.; Singh, I.; Ambekar, K.Distribution, and Fate of Emerging Persistent Organic Pollutants in the Environment. *In Management of Contaminants of Emerging Concern (CEC) in Environment*; Elsevier 2021169 .
(5) Ayala-Cabrera, J. F.; Santos, F. J.; Moyano, E. *Trends in Environmental Analytical Chemistry* **2021**, *30*, No. e00122.
(6) Focant, J.-F.; Sjödin, A.; Patterson, D. G. *Journal of Chromatography A* **2003**, *1019* (1−2), 143−156.
(7) Muscalu, A. M.; Górecki, T. *TrAC Trends in Analytical Chemistry* **2018**, *106*, 225−245.
(8) Hernández, F.; Sancho, J. V.; Ibáñez, M.; Abad, E.; Portolés, T.; Mattioli, L. *Anal Bioanal Chem.* **2012**, *403* (5), 1251−1264.
(9) Hernández, F.; Portolés, T.; Pitarch, E.; López, F. J. *TrAC Trends in Analytical Chemistry* **2011**, *30* (2), 388−400.
(10) Li, X.; Dorman, F. L.; Helm, P. A.; Kleywegt, S.; Simpson, A.; Simpson, M. J.; Jobst, K. J. *Molecules* **2021**, *26* (22), 6911.
(11) Ross, D. H.; Xu, L. *Anal. Chim. Acta* **2021**, *1154*, No. 338270.
(12) Metz, T. O.; Baker, E. S.; Schymanski, E. L.; Renslow, R. S.; Thomas, D. G.; Causon, T. J.; Webb, I. K.; Hann, S.; Smith, R. D.; Teeguarden, J. G. *Bioanalysis* **2017**, *9* (1), 81−98.
(13) Paglia, G.; Smith, A. J.; Astarita, G. *Mass Spectrom. Rev.* **2022**, *41* (5), 722−765.
(14) Gabelica, V. CHAPTER 1. Ion Mobility−Mass Spectrometry: An Overview. In *New Developments in Mass Spectrometry; Ashcroft, A. E.*, Sobott, F., Eds.; Royal Society of Chemistry: Cambridge, 2021; pp 1−25. DOI: 10.1039/9781839162886-00001.
(15) Izquierdo-Sandoval, D.; Fabregat-Safont, D.; Lacalle-Bergeron, L.; Sancho, J. V.; Hernández, F.; Portoles, T. *Anal. Chem.* **2022**, *94* (25), 9040−9047.
(16) Celma, A.; Sancho, J. V.; Schymanski, E. L.; Fabregat-Safont, D.; Ibáñez, M.; Goshawk, J.; Barknowitz, G.; Hernández, F.; Bijlsma, L. *Environ. Sci. Technol.* **2020**, *54* (23), 15120−15131.
(17) Regueiro, J.; Negreira, N.; Berntssen, M. H. G. *Anal. Chem.* **2016**, *88* (22), 11169−11177.
(18) Celma, A.; Ahrens, L.; Gago-Ferrero, P.; Hernández, F.; López, F.; Lundqvist, J.; Pitarch, E.; Sancho, J. V.; Wiberg, K.; Bijlsma, L. *Chemosphere* **2021**, *280*, No. 130799.
(19) Foster, M.; Rainey, M.; Watson, C.; Dodds, J. N.; Kirkwood, K. I.; Fernández, F. M.; Baker, E. S. *Environ. Sci. Technol.* **2022**, *56* (12), 9133−9143.
(20) Kirk, A. T.; Bohnhorst, A.; Raddatz, C.-R.; Allers, M.; Zimmermann, S. *Anal Bioanal Chem.* **2019**, *411* (24), 6229−6246.
(21) Delafield, D. G.; Lu, G.; Kaminsky, C. J.; Li, L. *TrAC Trends in Analytical Chemistry* **2022**, *157*, No. 116761.
(22) Dodds, J. N.; May, J. C.; McLean, J. A. *Anal. Chem.* **2017**, *89* (1), 952−959.
(23) Ridgeway, M. E.; Lubeck, M.; Jordens, J.; Mann, M.; Park, M. A. *Int. J. Mass Spectrom.* **2018**, *425*, 22−35.
(24) Giles, K.; Ujma, J.; Wildgoose, J.; Pringle, S.; Richardson, K.; Langridge, D.; Green, M. *Anal. Chem.* **2019**, *91* (13), 8564−8573.
(25) Garimella, S. V. B.; Nagy, G.; Ibrahim, Y. M.; Smith, R. D. *TrAC Trends in Analytical Chemistry* **2019**, *116*, 300−307.
(26) Larriba-Andaluz, C.; Prell, J. S. *Int. Rev. Phys. Chem.* **2020**, *39* (4), 569−623.
(27) Adams, K. J.; Montero, D.; Aga, D.; Fernandez-Lima, F. *Int. J. Ion Mobil. Spec.* **2016**, *19* (2−3), 69−76.
(28) Adams, K. J.; Smith, N. F.; Ramirez, C. E.; Fernandez-Lima, F. *Int. J. Mass Spectrom.* **2018**, *427*, 133−140.
(29) Adams, K. J.; Ramirez, C. E.; Smith, N. F.; Muñoz-Muñoz, A. C.; Andrade, L.; Fernandez-Lima, F. *Talanta* **2018**, *183*, 177−183.
(30) Jeanne Dit Fouque, K.; Ramirez, C. E.; Lewis, R. L.; Koelmel, J. P.; Garrett, T. J.; Yost, R. A.; Fernandez-Lima, F. *Anal. Chem.* **2019**, *91* (8), 5021−5027.
(31) Olanrewaju, C. A.; Ramirez, C. E.; Fernandez-Lima, F. *Anal. Chem.* **2021**, *93* (15), 6080−6087.
(32) Dodds, J. N.; May, J. C.; McLean, J. A. *Anal. Chem.* **2017**, *89* (1), 952−959.
(33) Zheng, X.; Dupuis, K. T.; Aly, N. A.; Zhou, Y.; Smith, F. B.; Tang, K.; Smith, R. D.; Baker, E. S. *Anal. Chim. Acta* **2018**, *1037*, 265−273.
(34) Wu, Q.; Wang, J.-Y.; Han, D.-Q.; Yao, Z.-P. *TrAC Trends in Analytical Chemistry* **2020**, *124*, No. 115801.
(35) Dodds, J. N.; Hopkins, Z. R.; Knappe, D. R. U.; Baker, E. S. *Anal. Chem.* **2020**, *92* (6), 4427−4435.
(36) Causon, T. J.; Hann, S. *Journal of Chromatography A* **2015**, *1416*, 47−56.
(37) MacNeil, A.; Li, X.; Amiri, R.; Muir, D. C. G.; Simpson, A.; Simpson, M. J.; Dorman, F. L.; Jobst, K. J. *Anal. Chem.* **2022**, *94* (31), 11096−11103.
(38) Aly, N. A.; Dodds, J. N.; Luo, Y.-S.; Grimm, F. A.; Foster, M.; Rusyn, I.; Baker, E. S. *Anal Bioanal Chem.* **2022**, *414* (3), 1245−1258.
(39) Mullin, L.; Jobst, K.; DiLorenzo, R. A.; Plumb, R.; Reiner, E. J.; Yeung, L. W. Y.; Jogsten, I. E. *Anal. Chim. Acta* **2020**, *1125*, 29−40.
(40) Goscinny, S.; Joly, L.; De Pauw, E.; Hanot, V.; Eppe, G. *Journal of Chromatography A* **2015**, *1405*, 85−93.
(41) Belova, L.; Caballero-Casero, N.; Van Nuijs, A. L. N.; Covaci, A. *Anal. Chem.* **2021**, *93* (16), 6428−6436.
(42) Silveira, J. A.; Ridgeway, M. E.; Laukien, F. H.; Mann, M.; Park, M. A. *Int. J. Mass Spectrom.* **2017**, *413*, 168−175.
(43) Dodds, J. N.; May, J. C.; McLean, J. A. *Anal. Chem.* **2017**, *89* (22), 12176−12184.
(44) Fernandez-Lima, F.; Kaplan, D. A.; Suetering, J.; Park, M. A. *Int. J. Ion Mobil. Spec.* **2011**, *14* (2−3), 93−98.
(45) Michelmann, K.; Silveira, J. A.; Ridgeway, M. E.; Park, M. A. *J. Am. Soc. Mass Spectrom.* **2015**, *26* (1), 14−24.
(46) Silveira, J. A.; Michelmann, K.; Ridgeway, M. E.; Park, M. A. *J. Am. Soc. Mass Spectrom.* **2016**, *27* (4), 585−595.
(47) Larriba-Andaluz, C.; Chen, X.; Nahin, M.; Wu, T.; Fukushima, N. *Anal. Chem.* **2019**, *91* (1), 919−927.
(48) Hernandez, D. R.; DeBord, J. D.; Ridgeway, M. E.; Kaplan, D. A.; Park, M. A.; Fernandez-Lima, F. *Analyst* **2014**, *139* (8), 1913−1921.
(49) Izquierdo-Sandoval, D.; Fabregat-Safont, D.; Lacalle-Bergeron, L.; Sancho, J. V.; Hernández, F.; Portoles, T. *Anal. Chem.* **2022**, *94* (25), 9040−9047.
(50) Focant, J.-F.; Eppe, G.; Pirard, C.; De Pauw, E. *Journal of Chromatography A* **2001**, *925* (1−2), 207−221.
(51) García-Bermejo, A.; Ábalos, M.; Sauló, J.; Abad, E.; González, M. J.; Gómara, B. *Anal. Chim. Acta* **2015**, *889*, 156−165.
(52) Benigni, P.; Fernandez-Lima, F. *Anal. Chem.* **2016**, *88* (14), 7404−7412.
(53) Benigni, P.; Porter, J.; Ridgeway, M. E.; Park, M. A.; Fernandez-Lima, F. *Anal. Chem.* **2018**, *90* (4), 2446−2450.
(54) Meier, F.; Brunner, A.-D.; Frank, M.; Ha, A.; Bludau, I.; Voytik, E.; Kaspar-Schoenefeld, S.; Lubeck, M.; Raether, O.; Bache, N.; Aebersold, R.; Collins, B. C.; Röst, H. L.; Mann, M. *Nat. Methods* **2020**, *17* (12), 1229−1236.
(55) Lesur, A.; Schmit, P.-O.; Bernardin, F.; Letellier, E.; Brehmer, S.; Decker, J.; Dittmar, G. *Anal. Chem.* **2021**, *93* (3), 1383−1392.
(56) Skowronek, P.; Krohs, F.; Lubeck, M.; Wallmann, G.; Itang, E. C. M.; Koval, P.; Wahle, M.; Thielert, M.; Meier, F.; Willems, S.; Raether, O.; Mann, M. *Molecular & Cellular Proteomics* **2023**, *22* (2), No. 100489.
(57) Dodds, J. N.; Alexander, N. L. M.; Kirkwood, K. I.; Foster, M. R.; Hopkins, Z. R.; Knappe, D. R. U.; Baker, E. S. *Anal. Chem.* **2021**, *93* (1), 641−656.

(58) Te Brinke, E.; Arrizabalaga-Larrañaga, A.; Blokland, M. H. *Anal. Chim. Acta* **2022**, *1222*, No. 340039.
(59) Dodds, J. N.; May, J. C.; McLean, J. A. *Anal. Chem.* **2017**, *89* (22), 12176−12184.
(60) van Leeuwen, S. P. J.; de Boer, J. *J. Chromatogr. A* **2008**, *1186* ((1−2)), 161−182.
(61) Muir, D.; Sverko, E. *Anal Bioanal Chem.* **2006**, *386* (4), 769−789.
(62) Deng, L.; Webb, I. K.; Garimella, S. V. B.; Hamid, A. M.; Zheng, X.; Norheim, R. V.; Prost, S. A.; Anderson, G. A.; Sandoval, J. A.; Baker, E. S.; Ibrahim, Y. M.; Smith, R. D. *Anal. Chem.* **2017**, *89* (8), 4628−4634.
(63) Chouinard, C. D.; Nagy, G.; Webb, I. K.; Shi, T.; Baker, E. S.; Prost, S. A.; Liu, T.; Ibrahim, Y. M.; Smith, R. D. *Anal. Chem.* **2018**, *90* (18), 10889−10896.
(64) May, J. C.; Leaptrot, K. L.; Rose, B. S.; Moser, K. L. W.; Deng, L.; Maxon, L.; DeBord, D.; McLean, J. A. *J. Am. Soc. Mass Spectrom.* **2021**, *32* (4), 1126−1137.
(65) Ma, Q.; Wang, C.; Bai, H.; Xi, H. W.; Xi, G. C.; Ren, X. M.; Yang, Y.; Guo, L. H. *J. Am. Soc. Mass Spectrom.* **2011**, *22* (10), s13361−011−0200−0202.
(66) Kajtazi, A.; Russo, G.; Wicht, K.; Eghbali, H.; Lynen, F. *Chemosphere* **2023**, *337*, No. 139361.
(67) Celma, A.; Bade, R.; Sancho, J. V.; Hernandez, F.; Humphries, M.; Bijlsma, L. *J. Chem. Inf. Model.* **2022**, *62* (22), 5425−5434.

https://doi.org/10.1021/acs.analchem.3c03039
Anal. Chem. 2023, 95, 17586−17594